An Experimental Study for the Effects of Noise on Pattern Recognition Algorithms

Guang Yi Chen and Adam Krzyzak

***Abstract* - Pattern recognition is a very important topic in computer vision. Among existing methods, which one is the most robust to noise? This is a very interesting question to answer. In this paper, we compare fifteen different methods for pattern recognition under different noise levels and different rotation angles. Most of these methods are invariant to translation, rotation, and scaling of the pattern images. Our experiments demonstrate that the Ridgelet + FFT (fast Fourier transform) descriptor is the most robust to additive Gaussian white noise (AGWN) for both a printed Chinese character dataset and an aircraft dataset. In addition, the Zernike moments and the Radon transform + FFT2 descriptor are also relatively robust to noise, but they are not as good as the Ridgelet + FFT descriptor for pattern recognition. We also compare the CPU (central processing units) computational time for all these methods for both pattern datasets.**

***Index Terms* - Pattern recognition; ridgelet transform; fast Fourier transform (FFT); discrete wavelet transform (DWT).**

I. INTRODUCTION

Pattern recognition is an extremely important research topic in today's computer vision applications. We briefly review several existing methods for pattern recognition here. Chen and Bui [1] proposed invariant Fourier-wavelet descriptor for pattern recognition. It polarizes the pattern image first, and then performs 1D discrete wavelet transform (DWT [2]) along the radial direction and the fast Fourier transform (FFT [3]) along the angle direction. The finally extracted features are invariant to the rotation of the pattern images. Khotanzad. and Hong [4] investigated invariant image recognition by Zernike moments. This method is very robust to additive Gaussian white noise for pattern recognition. Chen and Krzyzak [5] studied invariant pattern recognition with log-polar transform and dual-tree complex wavelet-Fourier features. Chen et al. [6] investigated rotation invariant feature extraction using ridgelet and Fourier transforms. The ridgelet transform performs the Radon transform first, and then the DWT along the radial direction. We conduct the FFT along the angle direction so that it is rotation invariant. Tang et al. [7] invented ring-projection-wavelet-fractal signatures: a novel approach to feature extraction. This method converts the patterns from 2D images to 1D signal, which is very fast in CPU computational time. Yin et al. [8] analyzed deep learning-aided OCR techniques for Chinese uppercase characters in the application of internet of things. Buoy et al. [9] studied toward a low-resource non-Latin-complete baseline to explore Khmer optical character recognition. Wu et al. [10] proposed a two-level rectification attention network for scene text recognition. Huang et al. [11] proposed a new approach for character recognition of multi-style vehicle license plates. Coquenet et al. [12] studied end-to-end handwritten paragraph text recognition using a vertical attention network. Xue et al. [13] proposed an image-to-character-to-word transformer for accurate scene text recognition.

In this paper, we study fifteen different methods for pattern recognition under different noise levels and different rotation angles. Most of these methods are invariant to translation, rotation, and scaling of the pattern images. Our experiments show that the Ridgelet + FFT method is the most robust to additive Gaussian white noise (AGWN) for both a printed Chinese character dataset and an aircraft dataset. Furthermore, the Zernike moments and the Radon transform + FFT2 descriptor are also relatively robust to noise, but they are not as good as the Ridgelet + FFT descriptor for pattern recognition. We also compare the CPU computational time for all fifteen methods for both a printed Chinese character dataset and an aircraft dataset.

The organization of this paper is given as follows. Section II briefly outlines fifteen existing pattern recognition algorithms. Section III performs some experiments to compare different algorithms for pattern recognition under noisy environment. Finally, Section IV concludes the paper and proposes future research directions.

II. PROPOSED STUDY

In this paper, we investigate which of the existing pattern recognition methods is the most robust to AGWN. We study fifteen methods in this paper, which are mostly rotation invariant to input pattern images. The translation and scaling invariance can be achieved by normalization techniques. The following fifteen methods are frequently used in today's pattern recognition tasks. We briefly summarize them as follows:

A. Center projection + dual-tree complex wavelet transforms (DTCWT [14]) + FFT. The center projection sums all pixels from the image centre to the

Manuscript received December 7, 2024; revised March 4, 2025.

Guang Yi Chen is an associate professor at Concordia University, Montreal, QC, Canada H3G 1M8. (Corresponding author, phone: +1 514 2715089, e-mail: guang_c@cse.concordia.ca).

Adam Krzyzak is a full professor at Concordia University, Montreal, QC, Canada H3G 1M8 (e-mail: krzyzak@cse.concordia.ca).

boundary along a line segment. We normalize the center project signal to have unit absolute sum. The DTCWT transform has the approximate shift invariant property, which is very important in pattern recognition. Furthermore, the FFT spectra are invariant to spatial shifts as well.

B. Center projection + FFT. We extract center projection first and then one dimensional FFT is applied to the center projection signal to extract rotation invariant features. The translation and scaling variance can be eliminated by standard normalization techniques.

C. Fourier- DWT descriptor [1]. It polarizes the pattern image, and then performs 1D DWT along the radial direction and the FFT along the angle direction. The finally extracted features are invariant to the rotation of the pattern images. The translation and scaling variance can be eliminated by standard normalization techniques.

D. Zernike Moments [4] are extracted from 2D images. These features are rotation invariant and relative noise robust. Zernike polynomials are an orthogonal basis set, which is a certain weighted average of the image pixels' intensities, usually chosen to have some attractive property or interpretation.

E. Line moments + DTCWT + FFT. The line moments are defined as the sum of the product of the radial distance from the pattern center with the pixel intensity. We normalize the line moment signal to have unit absolute sum. One dimensional DTCWT and FFT are applied to the line moments to extract multiresolution and rotation invariant features.

F. Line moments + FFT. We extract line moments first and then one dimensional FFT is applied to the line moment signal to extract rotation invariant features. The translation and scaling variance can be eliminated by standard normalization techniques.

G. Log-Polar transform. It converts the rotation and scaling factor from the original pattern image into spatial shifts in the log-polar domain, which is convenient for latter pattern recognition tasks.

H. Log-Polar + DTCWT + FFT2 [5]. We compute the 2D log-polar features first. Two dimensional DTCWT and FFT2 are then applied to the log-polar image to extract multiresolution and shift invariant features. This method extracts rotation and scaling invariant features from the pattern images.

I. Log-Polar + FFT2. We compute the 2D log-polar features first. Two dimensional FFT2 is then applied to the log-polar image to extract shift invariant features. This method extracts rotation and scaling invariant features from the pattern images.

J. Radon transform + FFT2. The Radon transform project the pattern image onto a line passing through the center of the pattern image. Two dimensional FFT2 is applied to the Radon image to extract shift invariant features. This method is relatively robust to AGWN for pattern recognition as demonstrated in the next section.

K. Ridgelet transform + FFT [6]. The ridgelet transform performs the Radon transform first, and then the DWT along the radial direction. We conduct the FFT along the angle direction so that it is rotation invariant. This method is very robust to AGWN for pattern recognition as shown in the next section. In addition, it is invariant to rotation of the pattern images due to the FFT transform.

L. Ring projection [7]. It sums all pixels on different circles centered at the image centroid with different radius. As a result, it is relatively robust to random noise. We normalize the ring project signal to have unit absolute sum. Nevertheless, the ring projection loses some recognition accuracy due to its conversion from 2D patterns into 1D signals. We are sacrificing some recognition accuracy in exchange for less processing time.

M. Ring projection + DTCWT + FFT. We compute the 1D ring projection signal first. One dimensional DTCWT and FFT are then applied to the ring projection signal to extract multiresolution and shift invariant features. This method extracts rotation invariant features from the pattern images. The translation and scaling variance can be eliminated by standard normalization techniques.

N. Ring projection + DWT + FFT. We compute the 1D ring projection signal first. One dimensional nonsubsampled DWT and FFT are then applied to the ring projection signal to extract multiresolution and shift invariant features. This method extracts rotation invariant features from the pattern images. The translation and scaling variance can be eliminated by standard normalization techniques.

O. Ring projection + FFT. We compute the 1D ring projection signal first. One dimensional FFT is then applied to the ring projection signal to extract shift invariant features. This method extracts rotation invariant features from the pattern images.

We can normalize the input pattern image so that it is translation and scaling invariant. Let the pattern image be $f(x,y)$ with M×N pixels. Define the moments with (p,q) order as

$$m_{pq} = \sum x^p y^q f(x,y). \tag{1}$$

The centroid of the aircraft is then calculated as

$$(\bar{x},\bar{y}) = (\frac{m_{10}}{m_{00}},\frac{m_{01}}{m_{00}}). \tag{2}$$

We can move this centroid to the center of the aircraft image. The scaling factor is computed as

$$\alpha = \sqrt{\beta / m_{00}}, \quad (3)$$

where β is a predefined constant. It is easy to prove that this normalization technique is approximately invariant to AGWN for translation, and it is exactly invariant to AGWN for scaling. We can also set the scaling factor as

$$\alpha = dim/(2 * dist), \quad (4)$$

where *dim=min(M,N)* and *dist* is the maximal distance from the centroid to the pattern boundary.

The main reason why we do not compare deep learning in this paper is because the number of classes in our pattern recognition problems can change frequently and the numbers of training samples are very limited. When new classes are available, we need to train the deep learning networks again, which is very time consuming. In addition, the number of patterns for each class should be large for deep learning, so collecting many training samples is a very difficult task. Existing pattern classification problems such as traffic sign recognition and handwritten digits recognition are good for deep learning since the numbers of classes in both problems do not change over time and the numbers of training samples are large. As a result, the pattern recognition algorithms compared in this paper are better suited for our classification problems since very limited numbers of training samples are available.

The major contributions of our new method can be given as follows. We compare fifteen different methods for pattern recognition under different noise levels and different rotation angles. Most of these methods are invariant to translation, rotation, and scaling of the pattern images. Our experiments demonstrate that the Ridgelet + FFT method is the most robust to AGWN for both a printed Chinese character dataset and an aircraft dataset. Furthermore, the Zernike moments and the Radon transform + FFT2 descriptor are also relatively robust to noise, but they are not as good as the Ridgelet + FFT descriptor for robust pattern recognition. Nevertheless, the Ridgelet + FFT method takes longer time to recognize a pattern compared than other existing methods. We are sacrificing more computing time in exchange for higher classification accuracy with this method. We can port it to a faster programming language such as C/C++ or Python. In addition, we can parallelize our code so that it can be executed much faster than before.

III. EXPERIMENTS

We conduct experiments on one printed Chinese character dataset with 85 characters of size 64×64 (see Fig. 1) and one aircraft dataset with 20 aircrafts of size 128×128 (see Fig. 2). All these pattern images are binary images. To add noise to pattern images, we scale all these binary images to the range of [0, 255]. We add AGWN to clean pattern image as follows:

$$g = f + \sigma_n N(0,1), \quad (5)$$

where g is the noisy image, f is the noise-free image, σ_n is the noise standard deviation, N(0,1) is the normal distribution with zero mean and unit variance. We fix the seed of the random number generator to zero such that we can generate the same experimental results for different runs. The noise standard deviation is set to (σ_n=30, 60, 90, 120, 150, 180, 210, 240, 270 and 300) in our experiments in this paper. Fig. 3 shows an illustration of noise patterns with σ_n=30, 60, 90, 120, 150, 180, 210, 240, 270 and 300 for a printed Chinese character. Fig. 4 shows an illustration of noise patterns with σ_n=30, 60, 90, 120, 150, 180, 210, 240, 270 and 300 for an aircraft. When noise levels are high, the pattern images can hardly be seen clearly due to noise. Nevertheless, some pattern recognition algorithms can still do an excellent job in recognizing them.

Our experiments conducted in this section have the following observations. Tables 1-3 show the correct recognition rates (%) with different algorithms and different noise levels (σ_n=30, 60, 90, 120, 150, 180, 210, 240, 270 and 300) for 30, 60 and 90 degrees of rotation for the printed Chinese character dataset, respectively. The best results are highlighted in bold font. The correct recognition rate is defined as the ratio between the number of correctly recognized patterns and the total number of patterns. The Ridgelet + FFT descriptor is the most robust to noise as can be seen from these three tables. In addition, Zernike moments is the second-best method. The Radon + FFT2 descriptor is the third best method, and the Fourier-DWT descriptor is the fourth best method for noise robust pattern recognition. All other methods are very sensitive to noise.

Tables 4-6 depict the correct recognition rates (%) with different algorithms and different noise levels (σ_n=30, 60, 90, 120, 150, 180, 210, 240, 270 and 300) for 30, 60 and 90 degrees of rotation for the aircraft dataset, respectively. The best results are highlighted in bold font. The Zernike Moments, the Radon + FFT2, the Ridgelet + FFT, and the Ring projection all achieve perfect classification accuracy (100%) for this dataset. By examining all six tables, we conclude that the Ridgelet + FFT descriptor is the most robust to noise as demonstrated in this paper. In addition, the Zernike moments and the Radon transform + FFT2 descriptor are also relatively robust to noise, but they are not as good as the Ridgelet + FFT descriptor for robust pattern recognition.

We measure the CPU time for all methods compared in this paper for both the printed Chinese dataset and the aircraft dataset. Our unoptimized Matlab code is run under the Linux operating system with Intel(R) Xeon(R) CPU E5-2697 v2 at 2.70GHz and 131 GB of random-access memory (RAM). Table 7 shows the execution time in seconds for all fifteen methods. The best results are highlighted in bold font. The fastest methods for both datasets are ring projection (L and O). Nevertheless, both methods achieve lower correct recognition rates for pattern recognition. Our method K achieves the highest correct recognition rates for pattern recognition for both the printed Chinese character dataset and the aircraft dataset, but it is the slowest in CPU time as shown in Table 7. We are sacrificing more computational time in exchange for high classification rates with this method. Even though our method K is a bit slow, it is not very slow in CPU time as can be seen from Table 7. Its speed is relatively fast as well for noise robust pattern recognition.

IV. CONCLUSIONS

Invariant pattern recognition is very important in many real-life applications. In this paper, we have studied which method is the most robust to AGWN for pattern recognition. We have compared fifteen existing pattern recognition methods with different noise levels and different rotation angles. Most of these methods are invariant to translation, rotation, and scaling of the pattern images. Our experiments demonstrate that the Ridgelet + FFT descriptor is the most robust to noise for pattern recognition with both a printed Chinese character dataset and an aircraft dataset. Furthermore, the Zernike moments and the Radon transform + FFT2 descriptor are also relatively robust to noise, but they are not as good as the Ridgelet + FFT descriptor for pattern recognition. Nevertheless, the Ridgelet + FFT method takes longer time to recognize a pattern compared than other existing methods. We are sacrificing more computing time in exchange for higher classification accuracy with this method.

Future research will be performed by studying deep convolutional neural networks (DCNN) for invariant pattern recognition. We can also perform a systematic study for other kinds of deformation such as skewing, illumination variation, occlusions, etc. for our invariant pattern recognition tasks.

REFERENCES

[1] G. Y. Chen and T. D. Bui, “Invariant Fourier-wavelet descriptor for pattern recognition,” Pattern Recognition, vol.32, pp.1083-1088, 1999.

[2] C. K. Chui, “An introduction to wavelets,” San Diego, CA: Academic Press, 1992.

[3] S. Bochner and K. Chandrasekharan, “Fourier Transforms,” Princeton University Press, 1949.

[4] A. Khotanzad. and Y. H. Hong, “Invariant image recognition by Zernike moments,” IEEE Transactions on Pattern Analysis and Machine Intelligence, vol. 12, pp. 489-497, 1990.

[5] G. Y. Chen and A. Krzyzak, “Invariant pattern recognition with log-polar transform and dual-tree complex wavelet-Fourier features,” Sensors, vol. 23, no. 8, 3842, 2023.

[6] G. Y. Chen, T. D. Bui and A. Krzyzak, “Rotation invariant feature extraction using ridgelet and Fourier transforms,” Pattern Analysis and Applications, vol. 9, no. 1, pp. 83-93, 2006.

[7] Y. Y. Tang, B. Li, H. Ma and J. Liu, “Ring-projection-wavelet-fractal signatures: a novel approach to feature extraction,” IEEE Trans. Circuits Systems II: Analog and Digital Signal Processing, vol. 45, no. 8, pp. 1130-1134, 1998.

[8] Y. Yin, W. Zhang, S. Hong, J. Yang, J. Xiong and G. Gui, “Deep Learning-Aided OCR Techniques for Chinese Uppercase Characters in the Application of Internet of Things,” IEEE Access, vol. 7, pp. 47043-47049, 2019.

[9] R. Buoy, M. Iwamura, S. Srun and K. Kise, “Toward a Low-Resource Non-Latin-Complete Baseline: An Exploration of Khmer Optical Character Recognition,” IEEE Access, vol. 11, pp. 128044-128060, 2023.

[10] L. Wu, Y. Xu, J. Hou, C. L. P. Chen and C. -L. Liu, “A Two-Level Rectification Attention Network for Scene Text Recognition,” IEEE Transactions on Multimedia, vol. 25, pp. 2404-2414, 2023.

[11] Q. Huang, Z. Cai and T. Lan, “A New Approach for Character Recognition of Multi-Style Vehicle License Plates,” IEEE Transactions on Multimedia, vol. 23, pp. 3768-3777, 2021.

[12] D. Coquenet, C. Chatelain and T. Paquet, “End-to-End Handwritten Paragraph Text Recognition Using a Vertical Attention Network,” IEEE Transactions on Pattern Analysis and Machine Intelligence, vol. 45, no. 1, pp. 508-524, 1 Jan. 2023.

[13] C. Xue, J. Huang, W. Zhang, S. Lu, C. Wang and S. Bai, “Image-to-Character-to-Word Transformers for Accurate Scene Text Recognition,” IEEE Transactions on Pattern Analysis and Machine Intelligence, vol. 45, no. 11, pp. 12908-12921, 1 Nov. 2023.

[14] N. G. Kingsbury, “Complex wavelets for shift invariant analysis and filtering of signals,” Journal of Applied and Computational Harmonic Analysis, vol. 10, pp. 234-253, 2001.

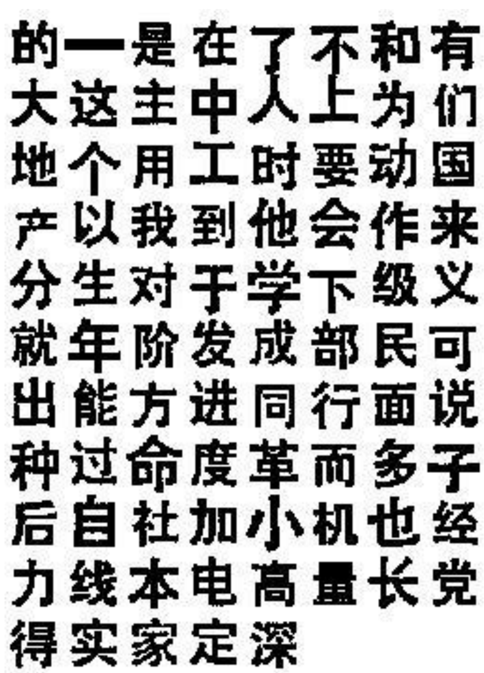

Fig. 1. The printed Chinese character dataset.

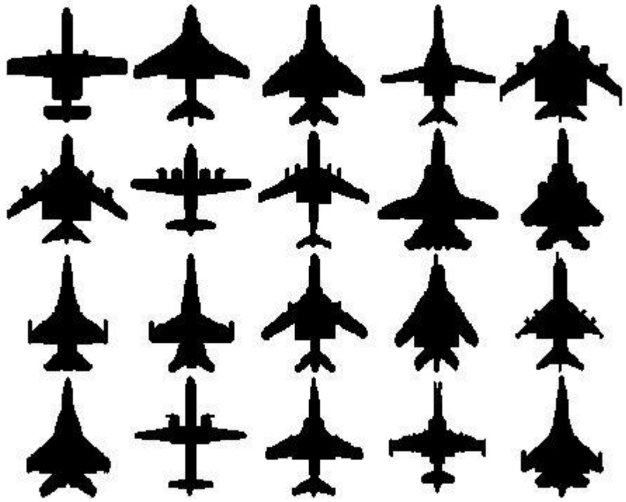

Fig. 2. The aircraft dataset.

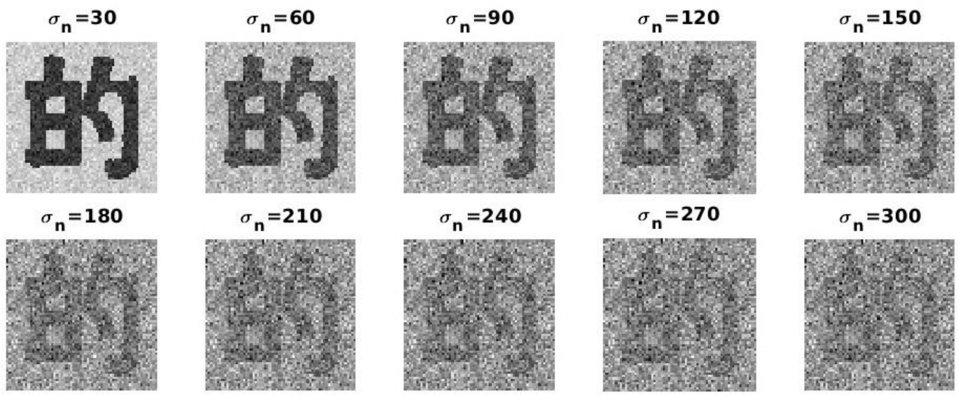

Fig. 3. An illustration of noise patterns with σ_n=30, 60, 90, 120, 150, 180, 210, 240, 270 and 300 for a printed Chinese character.

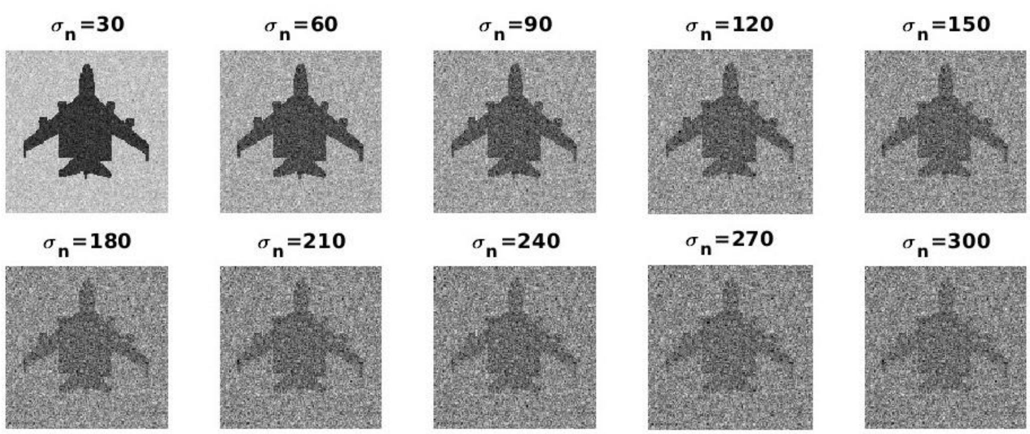

Fig. 4. An illustration of noise patterns with σ_n=30, 60, 90, 120, 150, 180, 210, 240, 270 and 300 for an aircraft.

TABLE 1
THE CORRECT RECOGNITION RATES (%) WITH DIFFERENT ALGORITHMS AND DIFFERENT NOISE LEVELS (Σ_N=30, 60, 90, 120, 150, 180, 210, 240, 270 AND 300) FOR 30 DEGREES OF ROTATION FOR THE PRINTED CHINESE CHARACTER DATASET. THE BEST RESULTS ARE HIGHLIGHTED IN BOLD FONT.

Method	**Noise σ_n**									
	30	60	90	120	150	180	210	240	270	300
A	98.8	98.8	97.6	78.8	67.1	45.9	32.9	29.4	24.7	17.6
B	**100**	**100**	**100**	94.1	78.8	58.8	48.2	36.5	25.9	18.8
C	**100**	**100**	**100**	**100**	**100**	98.8	96.5	85.9	69.4	61.2
D	**100**	**100**	**100**	**100**	**100**	**100**	**100**	98.8	96.5	89.4
E	98.8	**100**	90.6	52.9	31.8	10.6	7.1	4.7	2.4	2.4
F	**100**	**100**	97.6	62.4	27.1	15.3	7.1	3.5	3.5	3.5
G	28.2	24.7	10.6	9.4	8.2	7.1	8.2	8.2	5.9	5.9
H	**100**	98.8	84.7	38.8	12.9	8.2	4.7	3.5	2.4	2.4
I	**100**	98.8	22.4	15.3	0	0	0	0	0	0
J	**100**	**100**	**100**	100	100	100	98.8	96.5	95.3	87.1
K	**100**	**100**	**100**	**100**	**100**	**100**	**100**	**100**	**100**	**98.8**
L	**100**	**100**	**100**	92.9	78.8	67.1	56.5	47.1	36.5	35.3
M	82.4	37.6	22.4	24.7	21.2	11.8	3.5	4.7	5.9	4.7
N	84.7	54.1	32.9	22.4	16.5	12.9	8.2	5.9	2.4	1.1
O	78.8	43.5	29.4	24.7	16.5	11.8	5.9	3.5	2.4	1.2

TABLE 2
THE CORRECT RECOGNITION RATES (%) WITH DIFFERENT ALGORITHMS AND DIFFERENT NOISE LEVELS (Σ_N=30, 60, 90, 120, 150, 180, 210, 240, 270 AND 300) FOR 60 DEGREES OF ROTATION FOR THE PRINTED CHINESE CHARACTER DATASET. THE BEST RESULTS ARE HIGHLIGHTED IN BOLD FONT.

Method	**Noise σ_n**									
	30	60	90	120	150	180	210	240	270	300
A	**100**	97.6	94.1	82.4	64.7	48.2	36.5	29.4	22.4	18.8
B	**100**	**100**	97.6	90.6	76.5	56.5	41.2	32.9	22.4	17.6
C	**100**	**100**	**100**	**100**	**100**	98.8	94.1	78.8	71.8	62.4
D	**100**	**100**	**100**	**100**	**100**	98.8	96.5	96.5	90.6	83.5
E	**100**	**100**	85.9	48.2	22.4	5.9	3.5	2.4	1.2	2.4
F	**100**	**100**	97.6	65.9	24.7	8.2	2.4	1.2	0	0
G	7.1	4.7	1.2	1.2	1.2	0	0	0	0	0
H	**100**	98.8	83.5	34.1	15.3	5.9	4.7	2.4	2.4	2.4
I	**100**	95.3	23.5	12.9	0	0	0	0	1.2	1.2
J	**100**	**100**	**100**	**100**	**100**	98.8	98.8	96.5	89.4	77.6
K	**100**	**100**	**100**	**100**	**100**	**100**	**100**	**100**	**98.8**	**98.8**
L	**100**	**100**	96.5	90.6	82.4	74.1	63.5	44.7	41.2	37.6
M	80	36.5	28.2	24.7	20	11.8	5.9	4.7	5.9	4.7
N	83.5	52.9	36.5	24.7	16.5	14.1	9.4	5.9	4.7	2.4
O	76.5	44.7	30.6	24.7	17.6	7.1	5.9	3.5	2.4	2.4

TABLE 3
THE CORRECT RECOGNITION RATES (%) WITH DIFFERENT ALGORITHMS AND DIFFERENT NOISE LEVELS (Σ_N=30, 60, 90, 120, 150, 180, 210, 240, 270 AND 300) FOR 90 DEGREES OF ROTATION FOR THE PRINTED CHINESE CHARACTER DATASET. THE BEST RESULTS ARE HIGHLIGHTED IN BOLD FONT.

Method	**Noise σ_n**									
	30	60	90	120	150	180	210	240	270	300
A	**100**	**100**	98.8	91.8	68.2	45.1	37.6	25.9	17.6	12.9
B	**100**	**100**	**100**	95.3	82.4	56.5	43.5	34.1	23.5	14.1
C	**100**	**100**	**100**	**100**	**100**	**100**	97.6	89.4	81.2	72.9
D	**100**	**100**	**100**	**100**	**100**	**100**	97.6	96.5	95.3	89.4
E	**100**	**100**	**100**	81.2	40	29.4	14.1	11.8	3.5	3.5
F	**100**	**100**	98.8	82.4	44.7	21.2	11.8	7.1	5.9	3.5
G	7.1	5.9	1.2	1.2	1.2	1.2	1.2	1.2	0	0
H	**100**	**100**	98.8	80	40	20	10.6	4.7	3.5	2.4
I	**100**	98.8	29.4	16.5	0	0	0	0	0	0
J	**100**	**100**	**100**	**100**	**100**	**100**	98.8	96.5	87.1	77.6
K	**100**	**100**	**100**	**100**	**100**	**100**	**100**	**100**	**100**	**97.6**
L	100	100	100	98.8	92.9	83.5	71.8	65.9	50.6	40
M	97.6	56.5	42.4	40	29.4	12.9	7.1	5.9	5.9	3.5
N	96.5	68.2	44.7	30.6	18.8	11.8	10.6	3.5	1.2	1.2
O	97.6	52.9	43.5	34.1	16.5	11.8	4.7	2.4	2.4	2.4

TABLE 4
THE CORRECT RECOGNITION RATES (%) WITH DIFFERENT ALGORITHMS AND DIFFERENT NOISE LEVELS (Σ_N=30, 60, 90, 120, 150, 180, 210, 240, 270 AND 300) FOR 30 DEGREES OF ROTATION FOR THE AIRCRAFT DATASET. THE BEST RESULTS ARE HIGHLIGHTED IN BOLD FONT.

Method	**Noise σ_n**									
	30	60	90	120	150	180	210	240	270	300
A	**100**	**100**	**100**	**100**	95	95	90	80	80	70
B	**100**	**100**	**100**	**100**	95	95	85	85	85	80
C	**100**	**100**	**100**	**100**	**100**	**100**	**100**	**100**	**100**	**100**
D	**100**	**100**	**100**	**100**	**100**	**100**	**100**	**100**	**100**	**100**
E	**100**	95	60	25	10	5	5	5	5	5
F	**100**	95	60	20	15	5	5	5	5	5
G	10	10	10	10	10	5	5	5	5	5
H	**100**	**100**	95	50	20	15	5	5	5	5
I	**100**	**100**	60	20	15	15	5	5	5	5
J	**100**	**100**	**100**	**100**	**100**	**100**	**100**	**100**	**100**	**100**
K	**100**	**100**	**100**	**100**	**100**	**100**	**100**	**100**	**100**	**100**
L	**100**	**100**	**100**	**100**	**100**	**100**	**100**	**100**	**100**	**100**
M	90	50	30	30	25	30	35	30	15	10
N	**100**	**100**	**100**	**100**	**100**	**100**	95	95	85	75
O	**100**	**100**	**100**	**100**	**100**	**100**	95	95	90	80

TABLE 5
THE CORRECT RECOGNITION RATES (%) WITH DIFFERENT ALGORITHMS AND DIFFERENT NOISE LEVELS (Σ_N=30, 60, 90, 120, 150, 180, 210, 240, 270 AND 300) FOR 60 DEGREES OF ROTATION FOR THE AIRCRAFT DATASET. THE BEST RESULTS ARE HIGHLIGHTED IN BOLD FONT.

Method	**Noise σ_n**									
	30	60	90	120	150	180	210	240	270	300
A	**100**	**100**	**100**	**100**	**100**	**100**	**100**	90	90	90
B	**100**	**100**	**100**	**100**	**100**	**100**	**100**	**100**	95	90
C	**100**	**100**	**100**	**100**	**100**	**100**	**100**	**100**	**100**	**100**
D	**100**	**100**	**100**	**100**	**100**	**100**	**100**	**100**	**100**	**100**
E	**100**	95	45	20	15	5	5	5	5	5
F	**100**	**100**	50	20	20	10	10	5	5	5
G	10	10	10	10	10	10	10	10	5	5
H	**100**	**100**	**100**	60	20	20	10	10	5	5
I	**100**	**100**	90	20	15	15	15	10	5	5
J	**100**	**100**	**100**	**100**	**100**	**100**	**100**	**100**	**100**	**100**
K	**100**	**100**	**100**	**100**	**100**	**100**	**100**	**100**	**100**	**100**
L	**100**	**100**	**100**	**100**	**100**	**100**	**100**	**100**	**100**	**100**
M	85	40	25	30	30	30	40	20	15	10
N	**100**	**100**	**100**	**100**	**100**	**100**	95	90	85	75
O	**100**	**100**	**100**	**100**	**100**	**100**	95	90	90	80

TABLE 6
THE CORRECT RECOGNITION RATES (%) WITH DIFFERENT ALGORITHMS AND DIFFERENT NOISE LEVELS (Σ_N=30, 60, 90, 120, 150, 180, 210, 240, 270 AND 300) FOR 90 DEGREES OF ROTATION FOR THE AIRCRAFT DATASET. THE BEST RESULTS ARE HIGHLIGHTED IN BOLD FONT.

Method	**Noise σ_n**									
	30	60	90	120	150	180	210	240	270	300
A	**100**	**100**	**100**	**100**	**100**	**100**	**100**	90	80	80
B	**100**	**100**	**100**	**100**	**100**	**100**	**100**	90	85	85
C	**100**	**100**	**100**	**100**	**100**	**100**	**100**	**100**	**100**	95
D	**100**	**100**	**100**	**100**	**100**	**100**	**100**	**100**	**100**	**100**
E	95	95	45	15	10	5	5	5	5	5
F	**100**	95	40	20	5	5	5	5	5	5
G	25	25	20	20	20	20	20	20	20	15
H	**100**	**100**	**100**	65	25	20	15	10	5	5
I	**100**	**100**	85	25	15	15	15	10	10	5
J	**100**	**100**	**100**	**100**	**100**	**100**	**100**	**100**	**100**	**100**
K	**100**	**100**	**100**	**100**	**100**	**100**	**100**	**100**	**100**	**100**
L	**100**	**100**	**100**	**100**	**100**	**100**	**100**	**100**	**100**	**100**
M	**100**	40	30	25	30	30	50	30	15	15
N	**100**	**100**	**100**	**100**	**100**	95	95	95	80	75
O	**100**	**100**	**100**	**100**	**100**	**100**	**100**	**100**	95	85

TABLE 7
THE CPU TIME IN SECONDS FOR DIFFERENT METHODS AND FOR BOTH THE PRINTED CHINESE CHARACTER DATASET AND THE AIRCRAFT DATASET. THE BEST RESULTS ARE HIGHLIGHTED IN BOLD FONT.

Methods	Chinese Character Dataset	Aircraft Dataset
A	1.31	0.93
B	1.02	0.89
C	1.81	1.05
D	6.38	1.58
E	0.68	1.05
F	0.64	0.78
G	3.33	0.97
H	2.67	1.25
I	1.63	1.03
J	2.70	5.39
K	4.40	6.73
L	**0.18**	**0.79**
M	0.33	0.83
N	0.25	0.83
O	0.19	**0.79**

Guang Yi Chen holds a B.Sc. in Applied Mathematics, an M.Sc. in Computing Mathematics, an M.Sc. in Computer Science, and a Ph.D. in Computer Science. During his graduate and postdoctoral studies in Canada, he was awarded many prestigious fellowships. He has published over seventy journal papers in his fields and holds two granted US patents in image processing. He is currently affiliated to the Department of Computer Science and Software Engineering, Concordia University, Montreal, Quebec, Canada. He is the world's top 2% scientist ranked by Stanford University. He is also an IEEE Senior Member. His research interests include pattern recognition, image processing, machine learning, artificial intelligence, remote sensing, and scientific computing.

Adam Krzyzak received the M.Sc. and Ph.D. degrees in computer engineering from the Wrocław University of Science and Technology, Poland, in 1977 and 1980, respectively, and D.Sc. degree (habilitation) in computer engineering from the Warsaw University of Technology, Poland in 1998. In 2003 he received the Title of Professor from the President of the Republic of Poland. Since 1983, he has been with the Department of Computer Science and Software Engineering, Concordia University, Montreal, Canada, where he is currently a full professor. He published over 350 papers on neural networks, pattern recognition, nonparametric estimation, image processing, computer vision and control. He has been an associate editor of IEEE Transactions on Neural Networks and IEEE Transactions on Information Theory and is presently an Associate Editor-in-Chief of the Pattern Recognition Journal. He was co-editor of the book Computer Vision and Pattern Recognition (Singapore: World Scientific, 1989) and is a co-author of the book A Distribution-Free Theory of Nonparametric Regression, New York: Springer, 2002. He is a Fellow of the IEEE and a Fellow of IAPR